Relativistic effects in electron-energy-loss-spectroscopy observations of the Si/SiO_2 interface plasmon peak

P. Moreau
Cavendish Laboratory, Madingley Road, CB3 OHE Cambridge, England
and Laboratoire de Physique des Solides, Bâtiment 510, Université de Paris-Sud, F-91405, Orsay, France

N. Brun
Laboratoire de Physique des Solides, Bâtiment 510, Université de Paris-Sud, F-91405, Orsay, France

C. A. Walsh
Cavendish Laboratory, Madingley Road, CB3 OHE Cambridge, England

C. Colliex
Laboratoire de Physique des Solides, Bâtiment 510, Université de Paris-Sud, F-91405, Orsay, France

A. Howie
Cavendish Laboratory, Madingley Road, CB3 OHE Cambridge, England
(Received 21 March 1997)

Electron-energy-loss spectroscopy in a scanning transmission electron microscope has been used to study the interface plasmon peak (IPP) observed at the Si/SiO_2 interface. A precise line-spectrum recording shows a shift of the interface plasmon peak from 7.8 to 6.8 eV from the interface to 5 nm from it. This shift is explained by considering relativistic effects, demonstrating the importance of obtaining the relativistic formulas given in the two appendixes. The agreement of the simulations with the experiment, both in position and intensity is very good and is improved further by the introduction of a 1.0-nm-thick intermediate layer of SiO. A crystalline phase of SiO_2 seems to be in poorer agreement with experiment. This implies that the careful recording and simulation of the IPP can actually give some information about the nature of interfaces. [S0163-1829(97)06535-1]

I. INTRODUCTION

The Si/SiO_2 interface has been extensively studied in the past 10 years because of its influence on the performance of metal-oxide-semiconductor devices. Many different techniques have been applied in order to determine the structure and the properties of this interface. Among these, one can point out high-resolution electron microscopy (HREM),[1,2] x-ray photoemission spectroscopy,[3] Fresnel contrast,[4] and Auger electron spectroscopy.[5] Electron-energy-loss spectroscopy (EELS) in scanning transmission electron microscopes with high spatial resolution and chemical sensitivity, has also been used as a means of examining the energy-loss-near-edge structures,[6] extended energy-loss fine structure,[7] bulk and interface plasmons,[8] or just bulk plasmons.[9] They all agree in identifying an intermediate layer of approximately 1 nm of a material SiO_x $(x \leqslant 2)$ between the silicon and the silica parts.

The bulk and the interface plasmons are collective oscillations of the quasifree electrons in the material due to the penetrating fast electron.[10] The interface plasmon arises from the boundary conditions and is localized at the interface. Due to the use of an on-axis circular aperture, the spectra are recorded from quite low as well as high values of the scattering vector **k**. This prevents the shape and the position of the observed interface plasmon peak from being highly sensitive to the atomic scale structure of the interface.[11] This investigation of collective excitations must not be confused with changes that may occur in interband transition studies,[12] transitions that involve one electron processes. Nevertheless, the Si/SiO_2 interface is useful for testing theories in a sense that the interface plasmon peak appears clearly around 8 eV in the band gap of SiO_2 and in an energy domain where the Si EELS spectrum is low in intensity. We have thus chosen this example to show how precise the interpretation of this interface plasmon peak can be using dielectric theory. Furthermore, in many cases EELS is the only tool available for analyzing locally new materials like the nanoporous silicon involved in photoluminescence[13] or the macroporous silicon with a photonic band gap.[14]

Several authors[8,9,15] have found 8 ± 1 eV as the IPP position and the purpose of this paper is to show that this value can be much better defined and that relativistic effects must be taken into account in order to get a proper fit to the experiment.

II. EXPERIMENT

The experiments were carried out on thermally prepared Si/SiO_2 interfaces. A 140-nm-thick layer of SiO_2 has been grown on a Si (111) substrate. Thin sections for the electron microscope were obtained by the tripod polishing technique.[16]

EELS experiments were carried out at 100 kV with a VG

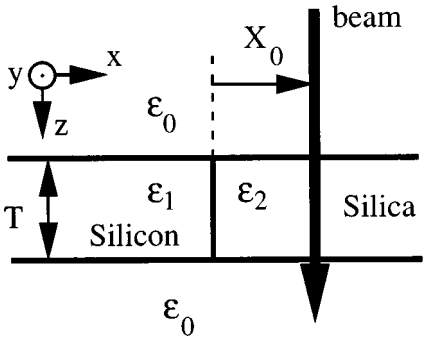

FIG. 1. Schematic view of the interface. The beam position is labeled as a function of x_0, the impact parameter.

HB501 FEG scanning transmission electron microscope. The data were collected at 0.10 eV/channel using a GATAN 666 PEELS spectrometer. The zero-loss-peak full width at half maximum (FWHM) was 0.7 eV. The spectra were recorded at 0.3-nm intervals across the interface using computer-controlled beam positioning (spectrum-line mode) (Fig. 1), each spectrum being acquired for 0.2 s. The estimated probe diameter was about 0.7 nm. The spectra were corrected for dark current and read-out noise using the GATAN supplied EL/P program. Deconvolution by the zero-loss-peak recorded in a hole of the grid was done using the PEELS program.[17] The spectra were reconvolved by a Gaussian of FWHM=0.6 eV to reduce the noise introduced by the deconvolution process.

Due to the varying diffraction conditions, the outgoing overall intensity analyzed by the spectrometer is not constant when crossing the interface. In order to compare with the calculated spectra, we have scaled each spectrum by dividing by the total number of counts from -10 to 90 eV and by the energy dispersion in order to obtain an intensity scale as a probability per eV. The result is substantially different from the raw data showing the necessity for recording the spectra on a large energy scale (Fig. 2). As we want to focus our interpretation on the interface plasmon peak around 8 eV an enlargement of Fig. 2 is presented in Fig. 3. The differences in given impact parameters are precise but their absolute values are not, i.e., the position of the interface is known only to an accuracy of ± 1 or 2 spectra (± 0.65 nm). The main observation is that this interface plasmon peak is shifted in energy from 7.8 to 6.8 eV when the impact parameter is, respectively, $x_0=-1$ and $+10$ nm. The reasons for this shift will be discussed below.

The objective and collector aperture were, respectively, 50 μm and 2 mm. Using the program CONCOR (Ref. 18) which corrects the collection angle for the effect of the convergence of the electron beam, we get an effective collection angle of 15 mrad. As the cutoff angle for silicon is approximately 7 mrad,[18] we have used this last value in the program BULK (Ref. 19) to fit the thickness T of our film. The dielectric constants for amorphous SiO_2 and crystalline Si have been extracted from optical measurements[20] using a 0.2-eV energy step. The best fit is found for $T=180\pm 10$ nm on both sides of the interface (see Fig. 4) with a good matching for the zero-loss peak, the first plasmon peak, and the second plasmon peak. It has, however, been necessary to multiply

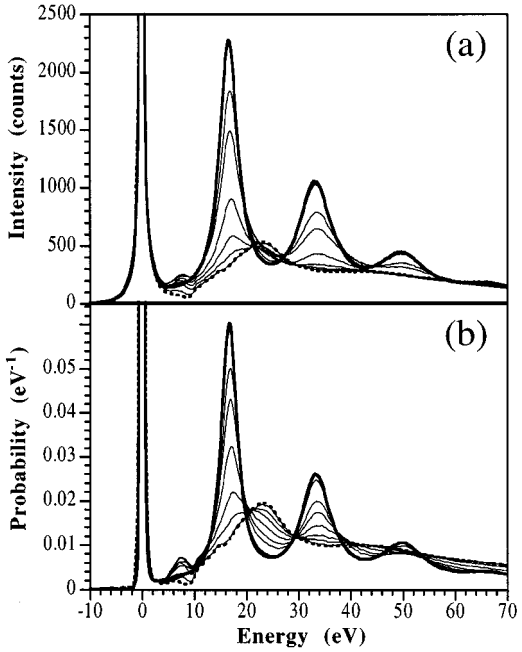

FIG. 2. (a) Raw experimental spectra. Only a few of the 128 recorded spectra are presented. The thicker line corresponds to $x_0=-10$ nm in the silicon and the thick dotted line to $x_0=+10$ nm in the silica. The thin lines are intermediate positions. (b) The experimental data after deconvolution with the zero-loss peak and rescaling of the total detected intensity. Same legend as in (a).

both experimental spectra by 1.1. The reason for this discrepancy is unknown but we are very confident with the thickness found since a Fourier-Log deconvolution of the experimental silicon spectrum gives $T/\lambda=1.58$ (λ total mean free path of the electron) which, combined with the value of λ [115 nm (Ref. 18)] leads to $T=180$ nm. As the value of T is the same on both sides of the interface, the thickness is constant across the interface. This check is essential for a proper comparison of the relative intensities when the interface is crossed.

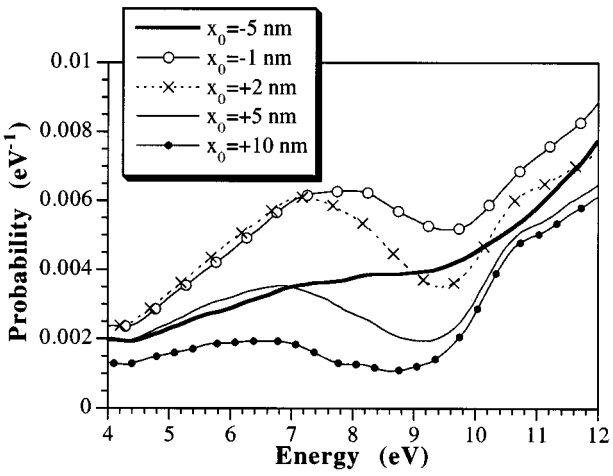

FIG. 3. Experimental interface plasmon peak spectra (magnification of Fig. 2), vs the impact parameter x_0.

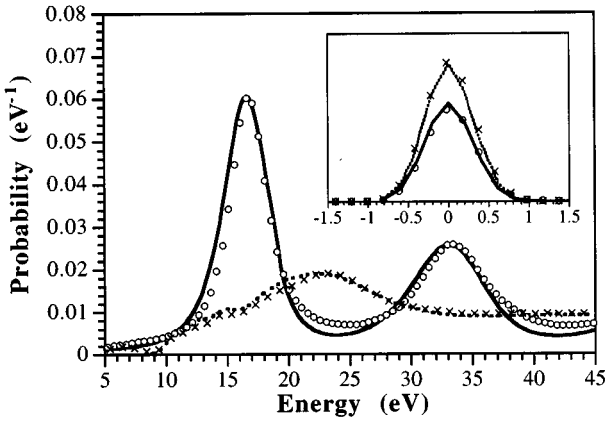

FIG. 4. Comparison of the experimental spectra for $x_0 = -10$ nm (○) in the silicon and $x_0 = +10$ nm (×) in the silica with multiple scattering calculations [(—) and (----), respectively]. The inset shows the zero-loss peak.

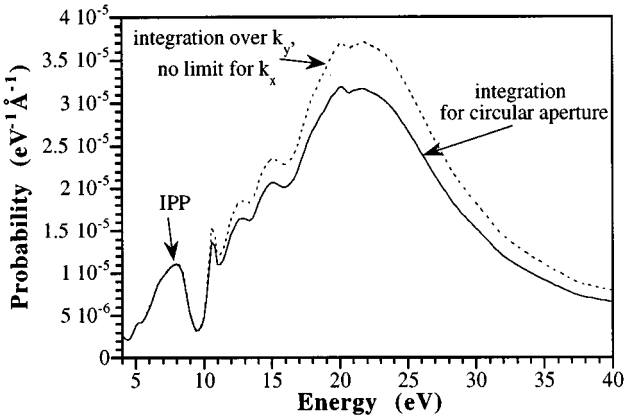

FIG. 5. Comparison of the theoretical excitation probabilities using formula (2) (----) and the formula given in Appendix A (—). Both calculations are done for $x_0 = +1.5$ nm.

Up to now, no analytical formulas have been established to describe the loss spectrum at an interface within a thin film, i.e., the surface plasmons on both top and bottom surfaces of the specimen have had to be considered separately from the interface plasmon. We have used the thickness determined above to compute the intensity of the surface plasmons applying Kröger's formula[21] for a uniform slab. This intensity is very small in the silica and contributes mainly with a smoothly varying shape around 11 eV in the silicon. Thus, this surface-plasmon intensity will not affect the interpretation below. Referring to this latter formula and to recent calculations,[22] one can assume that the coupling of the interface and surface plasmons is significant only for thicknesses below 30 nm. The rather large thickness of the sample studied here is then a valuable simplification in that sense.

Assuming pure elastic scattering by noncrystalline materials, simple Monte Carlo calculations[23] show that the broadening of the beam in the sample is approximately 10 nm in the silicon and in the silica for a 180-nm-thick film. Due to the collector aperture only $\frac{1}{4}$ of it is collected and so the area sampled is about 2.5 nm. This effect should be taken into account in addition to the finite size of the probe (0.5 nm) and the convergence of the beam. We assume that these are minor effects, only creating an overall broadening of the spectra because of the multiple x_0 values involved in each spectrum.

III. BASIC THEORY FOR INTERFACE PLASMON EXCITATIONS

The excitation probability P per unit path length and angular frequency ω is given by the nonrelativistic [formula (1)] and relativistic formulas[24] [formula (2)] below:

$$\frac{d^2P}{d\omega\, dz} = \frac{e^2}{2\pi^2 v^2 \varepsilon_0 \hbar}\,\mathrm{Im}\left\{\int_0^{k_{ym}} dk_y \left[-\frac{1}{\varepsilon_2 \nu} + \frac{1}{\varepsilon_2 \nu}\, e^{-2\nu x_0} + \frac{2e^{-2\nu x_0}}{\nu}\left\{-\frac{1}{\varepsilon_2+\varepsilon_1}\right\}\right]\right\}, \quad (1)$$

$$\frac{d^2P}{d\omega\, dz} = \frac{e^2}{2\pi^2 v^2 \varepsilon_0 \hbar}\,\mathrm{Im}\left\{\int_0^{k_{ym}} dk_y \left[-\frac{(1-\varepsilon_2\beta^2)}{\varepsilon_2 \nu_2} + \frac{(1-\varepsilon_2\beta^2)}{\varepsilon_2 \nu_2}\, e^{-2\nu_2 x_0} + 2e^{-2\nu_2 x_0}\left\{-\frac{1}{\varepsilon_2\nu_1+\varepsilon_1\nu_2} + \frac{\beta^2}{\nu_1+\nu_2}\right\}\right]\right\} \quad (2)$$

with

$$\nu = \sqrt{k_y^2+\omega^2/v^2}, \quad \nu_j = \sqrt{k_y^2+(\omega^2/v^2)(1-\varepsilon_j\beta^2)}$$

with a positive real part and $\beta = v/c$.

In both cases, the formula corresponds to an electron traveling in medium 2 (see Fig. 1). k_y is the component of the scattering vector along the y axis, ε_1 and ε_2 are the complex dielectric functions of the two media, v is the speed of the fast electron, x_0 is the impact parameter, e the elementary electrical charge, ε_0 the vacuum permittivity, $\hbar$ is Planck's constant, and c is the speed of light. Clearly recognizable are the usual terms $\mathrm{Im}(-1/\varepsilon_2)$, corresponding to the so-called bulk plasmon contribution, and $\mathrm{Im}[1/(\varepsilon_1+\varepsilon_2)]$ that give rise to the so-called interface plasmon peak. The exponential terms indicate that the intensity of the IPP is taken from the bulk one (the Begrenzung effect[10]) and vanishes for large impact parameters.

These formulas, extensively used in the present paper, perform the momentum integration for a finite k_y range, i.e., 0 to k_{ym}. k_x is implicitly integrated from 0 to infinity. However, this should not be so, since we have used a collector aperture limiting the scattering vector in both the x and y directions. We give in Appendix A the rigorous relativistic formula for a single interface. This formula has been used to calculate the excitation probability for a silicon/silica interface and a circular aperture corresponding to a cutoff angle of 7 mrad. Figure 5 shows the result for $x_0 = +1.5$ nm compared with the one obtained through formula (2). The intensity and position (between 3 and 10 eV) of the IPP are not affected by the introduction of a k_x limitation, due to its confinement in the y-z plane. However, the bulk-plasmon peak intensity is affected. As the purpose of this paper is to

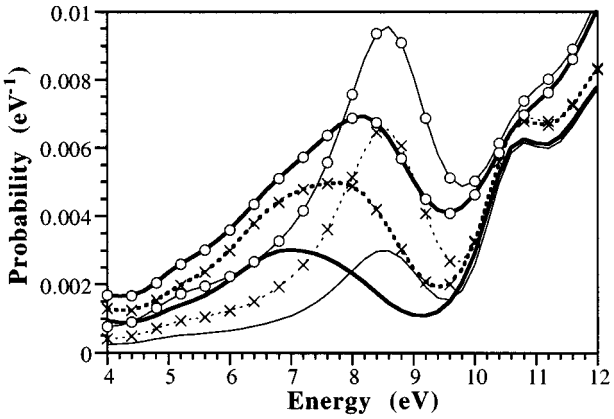

FIG. 6. Theoretical calculations of the intensities in the nonrelativistic case (thin lines) and in the relativistic case (thick lines). Three spectra for each case are shown [$x_0=-1$ nm (○), $x_0=+2$ nm (×), and $x_0=+5$ nm (—)].

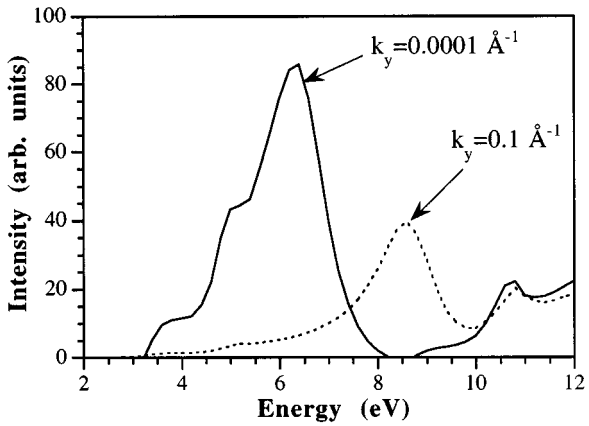

FIG. 7. The imaginary part of the relativistic surface-plasmon term for $k_y=0.1$ Å^{-1} (----) (multiplied by 50 for comparison) and $k_y=0.0001$ Å^{-1} (—).

focus on the IPP and because of the obvious greater simplicity of formula (2) over the one in Appendix A, we will use the former one to interpret our results.

IV. COMPARISON BETWEEN THEORY AND EXPERIMENT

Figure 6 compares the theoretical EEL spectra obtained for different impact parameters using the nonrelativistic formula (1) (thin lines) and the relativistic formula (2) (thick lines). The IPP is not shifted in energy in the nonrelativistic case. In formula (1), the term $\mathrm{Im}\{1/(\varepsilon_1+\varepsilon_2)\}$ can be extracted from the integral as in the local model, it does not depend on k_y. The integration over k_y (i.e., ν) will then, for each value of x_0, only be a scaling factor for $\mathrm{Im}\{1/(\varepsilon_1+\varepsilon_2)\}$. As this last term gives a peak at 8.5 eV, the IPP stays at 8.5 eV but decreases in intensity with increasing impact parameter.

The situation is very different in the relativistic case. The IPP is shifted to lower energies as the impact parameter is increased. This indicates that the only way to interpret the observed shift in a local dielectric model is to use a relativistic formula. It is thus essential to perform a relativistic calculation if one wants to extract information from interface plasmon peaks.

Calculations show that the $\beta^2/(\nu_1+\nu_2)$ term is negligible in the energy range 4–12 eV. Because of the finite speed of light, the energy of the interface plasmon is determined by the $1/(\nu_1\varepsilon_2+\varepsilon_1\nu_2)$ term [formula (2)]. Figure 7 shows the imaginary part of this term for two different values of k_y. For large values of k_y, one obtains a peak at 8.5 eV just as in the nonrelativistic case. This is because then $\nu_1\approx\nu_2\approx\nu$. Large values of k_y correspond in real space to small distance values; retardation effects are then insignificant. When k_y is small the term cannot be simplified and gives rise to a different resonance energy for the interface plasmon around 6 eV. The exponential term $\exp(-2\nu_2 x_0)$ also depends on k_y. When x_0 is small this term does not change much with k_y (Fig. 8) and the intensity comes from both relativistic and nonrelativistic interface plasmon peaks. We then get a peak around 8.5 eV and a shoulder around 7 eV. But, as x_0 increases, the high values of k_y become more and more unfavorable compared to small values and only the relativistic peak is then left. This is an obvious effect of retardation.

Relativistic effects may also explain why in small spherical silicon particles[25] one of the interface plasmon peaks is shifted from 4 eV when the spectrum is recorded with the beam going through the particle to 3 eV when the spectrum is recorded at grazing incidence. Furthermore, this explains also why the expected 8.7-eV position of the IPP for the Si/SiO_2 interface of the Si/SiO_2/Al/vacuum system in Ref. 15 is in fact observed at a lower energy.

However, the position of the IPP for an abrupt Si/SiO_2 interface is calculated to be 7.9 eV for $x_0=1.5$ nm whereas the experimental value is 7.2 eV. We have then introduced an intermediate layer of SiO between the silicon and the silica using optical dielectric data[20] and the formula given in Appendix B. The agreement with experiment is now quite good, both in the position of the peaks versus x_0 and in their intensities (compare Figs. 9 and 3). It has, however, been necessary to consider a small shift (0.5 nm) in the interface position, which is fairly reasonable. This calculation is presented for a $d=1$ nm wide SiO intermediate layer. Figure 10

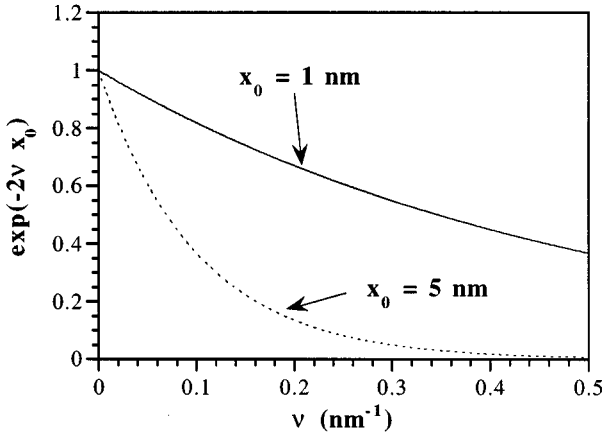

FIG. 8. The ν dependence of the exponential term for two x_0 values.

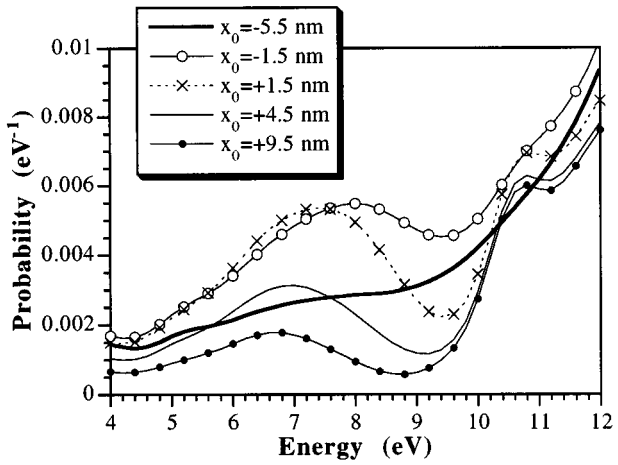

FIG. 9. Calculation of the interface plasmon peak with a $d = 1$ nm intermediate layer of SiO.

shows a comparison for $x_0 = 1.5$ nm between an experimental spectrum and calculations done for $d = 0.2$ nm, $d = 1$ nm, and $d = 2$ nm. The large intensity difference in the 10–30-eV energy range between experiment and theory results from the fact that the formula in Appendix B does not take into account the finite size of the aperture in the k_x direction (cf. Fig. 5 case). The three simulated spectra are very similar in the 10–30-eV energy range leading to a difficult discrimination between the three thicknesses. The energy of the IPP is far more sensitive to the thickness of the intermediate layer. It is shifted from 7.75 eV for $d = 0.2$ nm to 6.85 eV for $d = 2$ nm, the experimental value being 7.2 eV.

Ourmazd *et al.*[2] have deduced from HREM experiments that the intermediate layer was in fact a 0.5-nm-thick layer of tridymite, a crystalline phase of SiO_2. Unfortunately, no dielectric data are available for such a material. Nevertheless, between 0 and 10 eV the dielectric functions for the crystalline phase of SiO_2 are very similar;[26,27] we have then performed a calculation using the dielectric data of SiO_2

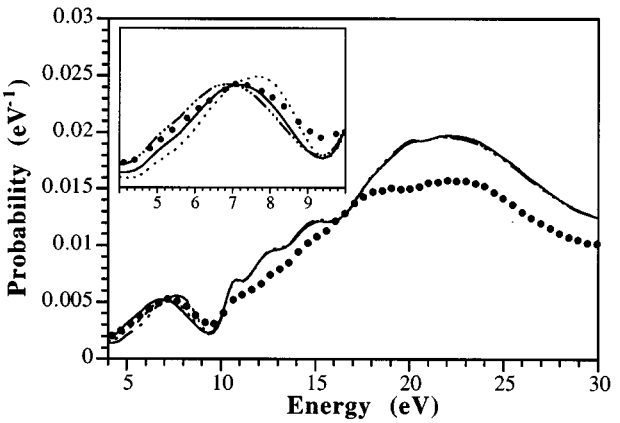

FIG. 10. Comparison of an experimental spectrum (●) with theoretical calculations for three different thicknesses of the SiO intermediate layer [$d = 0.2$ nm (----); $d = 1$ nm (—); $d = 2$ nm (···—···)]. All spectra are for $x_0 = +1.5$ nm.

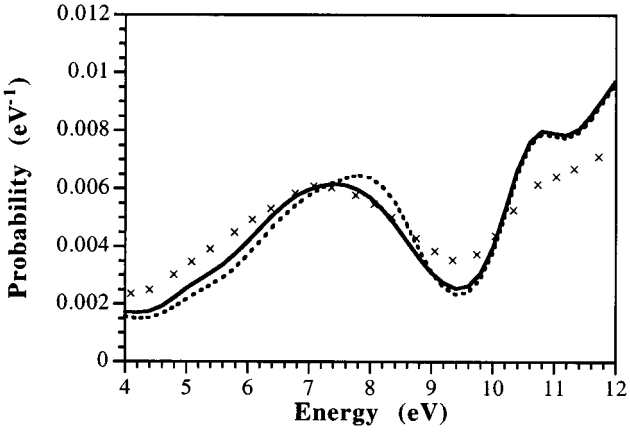

FIG. 11. Comparison of an experimental spectrum ($x_0 = +2$ nm, crosses) with two corresponding calculated spectra for a $d = 1$ nm SiO intermediate layer (—) and for a $d = 0.5$ nm SiO_2–α-quartz intermediate layer (----).

α-quartz.[20] Figure 11 shows an experimental spectrum for $x_0 = +2$ nm and the corresponding calculated spectra for an SiO intermediate layer and a crystalline SiO_2 intermediate layer (the discrepancy in the experimental and theoretical intensities around 11 eV are due both to the use of the noncircular aperture formula and the surface-plasmon excitation). The crystalline SiO_2 solution, because of the low sensitivity of the IPP to the chemistry of the interface, cannot be ruled out, but the calculated spectra display a poorer agreement with experiment compared with the SiO hypothesis.

V. CONCLUSION

The use of spectrum-line acquisition mode is essential for an accurate investigation of interface plasmons, and is, therefore, quite fruitful for an improved characterization of an interface, as demonstrated in the present case concerning the existence of an intermediate layer of SiO. It is also important to emphasize that a precise interpretation of plasmon losses is not possible without a consideration of the relativistic effects and one must be cautious about interpreting spectra whilst neglecting them. One could, however, either select large values of k_y by moving the collector aperture slightly off the optical axis and/or precisely positioning the beam on the interface where the relativistic peak is less favored. Finally, the agreement obtained between the experiment and the calculations proves that optical dielectric data are, to a very good approximation, suitable for understanding and simulating interface plasmon peaks.

ACKNOWLEDGMENTS

Financial support by EC TMR Grant No. ERB4001GT 00952239 is gratefully acknowledged. K. Yu-Zhang (Université de Marne la Vallée, France) and J. Rivory (Université Paris VI, France) are thanked for supplying the sample.

APPENDIX A: RELATIVISTIC EXPRESSION FOR THE EXCITATION PROBABILITY OF AN ELECTRON TRAVELING PARALLEL TO A PLANAR INTERFACE FOR A CIRCULAR APERTURE

Using a similar formalism to that described by Garcia Molina *et al.*,[24] one shows that the electrical field E_Z in the propagation direction of the beam at an impact parameter x_0 to the interface can be written as

$$E_z(z,k_y,\omega,x)=\chi_1 e^{\nu_1 x} \quad \text{for } x\leqslant 0,$$

$$E_z(z,k_y,\omega,x)=\chi_2 e^{-\nu_2 x}+\chi_3 e^{\nu_2 x} \quad \text{for } 0\leqslant x\leqslant x_0,$$

$$E_z(z,k_y,\omega,x)=(\chi_2+\chi_4)e^{-\nu_2 x} \quad \text{for } x\geqslant x_0,$$

with

$$\chi_1=\left(\frac{2\pi e}{v^2\varepsilon_2\nu_2}\frac{\omega}{i}\right)\frac{\varepsilon_2}{\varepsilon_1}\frac{2\nu_2}{\nu_2+\nu_1}\left\{(1-\varepsilon_1\beta^2)-\frac{\nu_1(\varepsilon_2-\varepsilon_1)}{\nu_1\varepsilon_2+\nu_2\varepsilon_1}\right\}e^{-\nu_2 x_0+i\omega z/v},$$

$$\chi_2=\left(\frac{2\pi e}{v^2\varepsilon_2\nu_2}\frac{\omega}{i}\right)\frac{1}{\nu_2+\nu_1}\left\{\frac{2\nu_2^2(\varepsilon_2-\varepsilon_1)}{\nu_2\varepsilon_1+\nu_1\varepsilon_2}+(1-\beta^2\varepsilon_2)(\nu_2-\nu_1)\right\}e^{-\nu_2 x_0+i\omega z/v},$$

$$\chi_3=\left(\frac{2\pi e}{v^2\varepsilon_2\nu_2}\frac{\omega}{i}\right)(1-\beta^2\varepsilon_2)e^{-\nu_2 x_0+i\omega z/v},$$

$$\chi_4=\left(\frac{2\pi e}{v^2\varepsilon_2\nu_2}\frac{\omega}{i}\right)(1-\beta^2\varepsilon_2)e^{+\nu_2 x_0+i\omega z/v},$$

where

$$\nu_i^2=k_y^2+\frac{\omega^2}{v^2}(1-\beta^2\varepsilon_i), \quad \mathrm{Re}(\nu_i)\geqslant 0, \quad \beta=v/c,$$

ε_1, ε_2 are the dielectric constants of the two media, v is the fast electron speed, c the speed of light, e the elementary electrical charge, and ω the angular frequency.

Hence, using the Heaviside function, E_z can be written as

$$E_z(z,k_y,\omega,x)=\chi_1 e^{\nu_1 x}H(-x)+(\chi_2 e^{-\nu_2 x}+\chi_3 e^{\nu_2 x})H(x)H(x_0-x)+(\chi_2+\chi_4)e^{-\nu_2 x}H(x-x_0).$$

In order to integrate over k_x and k_y, one must perform the following Fourier transform:

$$E_z(z,k_y,\omega,k_x)=\int_{-\infty}^{\infty}E_z(z,k_y,\omega,x)e^{-ik_x x}dx.$$

Then, evaluating E_z at x_0:

$$E_z(z,x_0)=\int_{-\infty}^{\infty}\frac{dk_y}{2\pi}\int_{-\infty}^{\infty}\frac{dk_x}{2\pi}\int_{-\infty}^{\infty}\frac{d\omega}{2\pi}e^{ik_x x_0-i\omega t}\times E_z(z,k_y,\omega,k_x).$$

The retarding force at the particle is equal to its energy-loss per unit path length, so

$$\frac{dW}{dz}=eE_z(z=vt,x_0)$$

and as

$$\frac{dW}{dz}=-\int_0^{\infty}\frac{d^2P}{dz\,d\omega}\hbar\omega\,d\omega$$

[(Ref. 10)], we get, for a circular aperture defining a cutoff vector q_c, the probability of excitation of an angular frequency ω per unit path length and per unit frequency

$$\frac{d^2P}{dz\,d\omega}=-\mathrm{Im}\left(\int_0^{q_c}dk_y\lambda_0\int_0^{(q_c^2-k_y^2)^{1/2}}dk_x\left\{\frac{\lambda_1\nu_1\cos(k_x x_0)}{\nu_1^2+k_x^2}-\frac{\lambda_1 k_x\sin(k_x x_0)}{\nu_1^2+k_x^2}+\frac{(\lambda_2-\lambda_3)\nu_2\cos(k_x x_0)}{\nu_2^2+k_x^2}+\frac{(\lambda_2+\lambda_3)k_x\sin(k_x x_0)}{\nu_2^2+k_x^2}+\frac{2\lambda_3\nu_2 e^{\nu_2 x_0}}{\nu_2^2+k_x^2}\right\}\right)$$

with

$$\lambda_0=\frac{e^2}{2\pi^3\varepsilon_0\varepsilon_2 v^2\nu_2\hbar},$$

$$\lambda_1=\frac{\varepsilon_2}{\varepsilon_1}\frac{2\nu_2}{\nu_2+\nu_1}\left\{(1-\varepsilon_1\beta^2)-\frac{\nu_1(\varepsilon_2-\varepsilon_1)}{\nu_1\varepsilon_2+\nu_2\varepsilon_1}\right\}e^{-\nu_2 x_0},$$

$$\lambda_2=\frac{1}{\nu_2+\nu_1}\left\{\frac{2\nu_2^2(\varepsilon_2-\varepsilon_1)}{\nu_2\varepsilon_1+\nu_1\varepsilon_2}+(1-\beta^2\varepsilon_2)(\nu_2-\nu_1)\right\}e^{-\nu_2 x_0},$$

and

$$\lambda_3=(1-\beta^2\varepsilon_2)e^{-\nu_2 x_0}.$$

APPENDIX B: RELATIVISTIC EXPRESSION FOR THE EXCITATION PROBABILITY OF AN ELECTRON TRAVELING PARALLEL TO A SANDWICH INTERFACE, INTEGRATION LIMITED ONLY IN THE k_y DIRECTION

We consider a double planar interface between three media with dielectric functions ε_1, ε_2, and ε_3. x_0 is the impact parameter of the electrons from the center of the intermediate layer and d is the thickness of the intermediate layer. k_{ym} is the maximum scattered wave number.

Following the same general idea as the one described in Ref. 24 but now for a double interface and using the same relations and definitions as in Appendix A, one finally obtains for $x_0\geqslant d/2$,

$$\frac{d^2P}{d\omega\, dz}=\frac{e^2}{2\pi^2v^2\varepsilon_0\hbar}\,\mathrm{Im}\left(\int_0^{k_{ym}}dk_y\left\{\frac{-(1-\beta^2\varepsilon_3)}{\nu_3\varepsilon_3}+\frac{(1-\beta^2\varepsilon_3)}{\varepsilon_3}\,\Gamma+\Lambda\,\exp\left[-\nu_3\left(x_0-\frac{d}{2}\right)\right]\right\}\right),$$

where

$$\Gamma=\frac{\exp\left[-2\nu_3\left(x_0-\frac{d}{2}\right)\right]}{\nu_3}-\frac{2\,\exp\left[-2\nu_3\left(x_0-\frac{d}{2}\right)\right]}{J}\{(\nu_2+\nu_1)\exp(\nu_2d)+(\nu_2-\nu_1)\exp(-\nu_2d)\},$$

$$J=(\nu_1+\nu_2)(\nu_3+\nu_2)\exp(\nu_2d)+(\nu_3-\nu_2)(\nu_2-\nu_1)\exp(-\nu_2d),$$

$$\Lambda=\frac{1}{JL}\left[8\nu_3\nu_2^2(\varepsilon_1-\varepsilon_2)\exp\left\{-\nu_3\left(x_0-\frac{d}{2}\right)\right\}+\frac{2\nu_3}{\varepsilon_3}(\varepsilon_2-\varepsilon_3)\exp\left\{-\nu_3\left(x_0-\frac{d}{2}\right)\right\}\{(\nu_1\varepsilon_2+\nu_2\varepsilon_1)\exp(\nu_2d)\right.$$

$$\left.+(\nu_2\varepsilon_1-\nu_1\varepsilon_2)\exp(-\nu_2d)\}\{(\nu_1+\nu_2)\exp(\nu_2d)+(\nu_2-\nu_1)\exp(-\nu_2d)\}\right],$$

$$L=[(\nu_3\varepsilon_2+\nu_2\varepsilon_3)(\nu_2\varepsilon_1+\nu_1\varepsilon_2)\exp(\nu_2d)+(\nu_2\varepsilon_1-\nu_1\varepsilon_2)(\nu_3\varepsilon_2-\nu_2\varepsilon_3)\exp(-\nu_2d)].$$

$$\nu_i=\left\{k_y^2+\frac{\omega^2}{v^2}(1-\beta^2\varepsilon_i)\right\}^{1/2}$$

with a positive real part.

Similarly for $0\leqslant x_0\leqslant d/2$,

$$\frac{d^2P}{d\omega\, dz}=\frac{e^2}{2\pi^2v^2\varepsilon_0\hbar}\,\mathrm{Im}\left(\int_0^{k_{ym}}\frac{dk_y}{\nu_2\varepsilon_2}\left\{-(1-\beta^2\varepsilon_2)-(1-\beta^2\varepsilon_2)\,\frac{T}{J}+\frac{Y}{J.L}\right\}\right),$$

where J and L are as defined above and

$$T=(\nu_2+\nu_1)(\nu_2-\nu_3)\exp(2\nu_2x_0)+(\nu_2-\nu_1)(\nu_2+\nu_3)\exp(-2\nu_2x_0)-2(\nu_1-\nu_2)(\nu_2-\nu_3)\exp(-\nu_2d),$$

$$Y=2\nu_2^2\left\{(\nu_2\varepsilon_1+\nu_1\varepsilon_2)(\nu_1+\nu_2)(\varepsilon_3-\varepsilon_2)\exp\left[2\nu_2\left(x_0+\frac{d}{2}\right)\right]+(\nu_1\varepsilon_2-\nu_2\varepsilon_1)(\nu_2-\nu_1)(\varepsilon_3-\varepsilon_2)\exp\left[-2\nu_2\left(x_0+\frac{d}{2}\right)\right]\right.$$

$$+(\nu_3\varepsilon_2-\nu_2\varepsilon_3)(\nu_2-\nu_3)(\varepsilon_1-\varepsilon_2)\exp\left[2\nu_2\left(x_0-\frac{d}{2}\right)\right]+(\nu_2\varepsilon_3+\nu_3\varepsilon_2)(\nu_2+\nu_3)(\varepsilon_1-\varepsilon_2)\exp\left[-2\nu_2\left(x_0-\frac{d}{2}\right)\right]$$

$$\left.+2\nu_2(\nu_3+\nu_1)(\varepsilon_1-\varepsilon_2)(\varepsilon_2-\varepsilon_3)\right\}.$$

[1] O. L. Krivanek, T. T. Sheng, and D. C. Tsui, Appl. Phys. Lett. **32**, 437 (1978).

[2] A. Ourmazd, D. W. Taylor, J. A. Rentschlera, and J. Bevk, Phys. Rev. Lett. **59**, 213 (1987).

[3] P. J. Grunthaner, M. H. Hecht, F. J. Grunthaner, and N. M. Johnson, J. Appl. Phys. **61**, 629 (1987).

[4] F. M. Ross and W. M. Stobbs, Philos. Mag. A **63**, 1 (1991).

[5] J. F. Wager and C. W. Wilmsen, J. Appl. Phys. **50**, 874 (1979).

[6] P. E. Batson, Nature (London) **366**, 727 (1993).

[7] Z. W. Yuan, S. Csillag, M. A. Tafreshi, and C. Colliex, Ultramicroscopy **59**, 149 (1995).

[8] M. G. Walls and A. Howie, Ultramicroscopy **28**, 40 (1989); M. G. Walls, Ph.D. thesis, University of Cambridge, England, 1988.

[9] H. Fukuda, M. Yasuda, and T. Iwabuchi, Appl. Phys. Lett. **61**, 693 (1992).

[10] R. H. Ritchie, Phys. Rev. **106**, 874 (1957).

[11] A. Howie and R. H. Milne, J. Microsc. **136**, 279 (1984).

[12] H. Müllejans and R. H. French, J. Phys. D **29**, 1751 (1996).

[13] A. Albu-Yaron, S. Bastide, D. Bouchet, N. Brun, C. Colliex, and C. Lévy-Clément, J. Phys. I **4**, 1181 (1994); L. N. Dinh, L. L. Chase, M. Balooch, W. J. Siekhaus, and F. Wooten, Phys. Rev. B **54**, 5029 (1996); I. Berbezier, J. M. Martin, C. Bernardi, and J. Derrien, Appl. Surf. Sci. **102**, 417 (1996).

[14] U. Grüning, V. Lehmann, S. Ottow, and K. Busch, Appl. Phys. Lett. **68**, 747 (1996).

[15] M. A. Turowski, T. F. Kelly, and P. E. Batson, J. Appl. Phys. **76**, 3776 (1994).

[16] J. Ayache and P. H. Albarède, Ultramicroscopy **60**, 195 (1995).

[17] P. Fallon and C. A. Walsh, Parallel Electron Energy Loss Spectroscopy (PEELS) program (University of Cambridge, England, 1996).

[18] R. F. Egerton, *Electron Energy Loss Spectroscopy in the Electron Microscope*, 2nd ed. (Plenum, New York, 1996).

[19] C. A. Walsh, *Computer Programs for the Calculation of Electron Energy-Loss Spectra from Interfaces Between Dielectric Media* (Cavendish Laboratory, Cambridge, 1992).

[20] *Handbook of Optical Dielectric Constants of Solids*, edited by D. Palik (Naval Research Laboratory, Washington, D.C., 1985).

[21] E. Kröger, Z. Phys. **235**, 403 (1970).
[22] A. Rivacoba, N. Zabala, and P. M. Echenique, Phys. Rev. Lett. **69**, 3362 (1992); J. Aizpurua (private communication).
[23] D. C. Joy, *Monte Carlo Simulations of Electron Beam-Solid Interactions in Monte Carlo Modeling for Electron Microscopy and Microanalysis* (Oxford University Press, New York, 1995).
[24] R. Garcia Molina, A. Gras Marti, A. Howie, and R. H. Ritchie, J. Phys. C **18**, 5335 (1985).
[25] D. Ugarte, C. Colliex, and P. Trebbia, Phys. Rev. B **45**, 4332 (1992).
[26] D. W. McComb and A. Howie, Nucl. Instrum. Methods Phys. Res. B **96**, 569 (1995).
[27] Y. Xu and W. Y. Ching, Phys. Rev. B **44**, 11 048 (1991).